



Magnetic circular polarization of luminescence in bismuth-doped silica glass

Oleksii Laguta, Hicham El Hamzaoui, Mohamed Bouazaoui, Vladimir Arion,
And Igor Razdobreev

► To cite this version:

Oleksii Laguta, Hicham El Hamzaoui, Mohamed Bouazaoui, Vladimir Arion, And Igor Razdobreev. Magnetic circular polarization of luminescence in bismuth-doped silica glass. *Optica*, 2015, 2 (8), pp.663. 10.1364/OPTICA.2.000663 . hal-01187480

HAL Id: hal-01187480

<https://hal.science/hal-01187480>

Submitted on 8 Jan 2024

HAL is a multi-disciplinary open access archive for the deposit and dissemination of scientific research documents, whether they are published or not. The documents may come from teaching and research institutions in France or abroad, or from public or private research centers.

L'archive ouverte pluridisciplinaire **HAL**, est destinée au dépôt et à la diffusion de documents scientifiques de niveau recherche, publiés ou non, émanant des établissements d'enseignement et de recherche français ou étrangers, des laboratoires publics ou privés.

Magnetic circular polarization of luminescence in Bismuth-doped silica glass

Oleksii Laguta,¹ Hicham El Hamzaoui,² Mohamed Bouazaoui,² Vladimir B. Arion,³ and Igor Razdobreev^{1, a)}

¹⁾*CERLA, PHLAM UMR CNRS 8523, University Lille 1, 59655 Villeneuve d'Ascq,*

France

²⁾*IRCICA - UMR8523/FR3024 CNRS, Parc de la Haute Borne, 50 av. Halley, 59658 Villeneuve d'Ascq,*

France

³⁾*Institute of Inorganic Chemistry, University of Vienna, Waehringer Str. 42, A-1090 Vienna, Austria*

(Dated: 6 July 2021)

The magnetic field induced circular polarization of near infrared photoluminescence in Bi-doped pure silica glass was studied in the spectral range of 660-1600nm covering three excited state levels. The highest degree of magnetic circular polarization of luminescence was observed in the lasing, first excited state (peak emission at 1440 nm). The results of variable temperature and variable magnetic field measurements allows to conclude that the near infrared luminescence originates from an isolated non-Kramers doublet of the even-electron system.

Over the past decade there has been increasing interest in the development of Bi-doped fibre lasers (BFL) and amplifiers (BFA). Despite the significant progress achieved in recent years¹, such devices suffer from a number of drawbacks. The very low levels of Bismuth doping and, as a consequence, significant fiber length (typically 80-100 m) are necessary to ensure the efficient BFL and BFA operation. Also, the efficiency of the BFL and BFA remains significantly lower in comparison to their rare earth counterparts. Unfortunately, the poor understanding of the nature of near-infrared (NIR) photoluminescence (PL) in Bi-doped glasses does not allow the development of efficient devices. Indeed, since the first demonstration of the NIR PL in Bi-doped silica glasses^{2,3} and up to now the nature of the NIR PL in Bi-doped glasses remains a subject of debates^{4,5}. In this context new experiments are necessary to clarify the nature of luminescent centers in Bi-doped silica glasses.

It is well known^{6,7} that the magnetic circular dichroism (MCD) and closely related magnetic circular polarization of luminescence (MCPL) are universal techniques for investigation of the paramagnetic impurities when the detection of the electron spin resonance (ESR) becomes difficult or even impossible. Both effects are considered as a sum of the contributions from the so-called \mathcal{A} , \mathcal{B} and \mathcal{C} terms, originally introduced by R. Serber⁸. The only temperature dependent and purely paramagnetic term \mathcal{C} is due to the Boltzmann population distribution among the Zeeman-split sublevels. The diamagnetic term \mathcal{B} is due to the magnetic field (MF) mixing between a degenerate level (initial) and another one (excited, ground or even itself). Finally, the term \mathcal{A} , also called diamagnetic, is caused by the difference in the energies of the final states (excited in MCD and "ground" in MCPL). In the present Letter we report on the MCPL in Bi-doped silica without other co-dopant. The choice of the MCPL technique is due to the very low absorption in the NIR

spectral region and our preference for the bulk samples with Bismuth content as close as possible to the core of lasing fiber. For the first time we show that some of the luminescence bands in the Bi-doped silica glass are the magnetic multiplets. The degree of MCPL is defined as $\Delta_{\text{MCPL}} = (I^+ - I^-)/I_{\text{tot}}$, where $I_{\text{tot}} = (I^+ + I^-)$, I^+ and I^- are the intensities of σ^+ and σ^- components, respectively. The highest degree of MCPL was found in the luminescence from the lowest, lasing excited state (ES). At $\lambda_{\text{em}} = 1440 \text{ nm}$ corresponding to the NIR PL maximum at 1.48 K and in the MF of 6 T we measured $\Delta_{\text{MCPL}} \approx 0.28$.

The samples of silica glasses were produced following the technique described previously⁹. At the first step the nanoporous silica xerogel in the form of cylindrical rod with an average pore diameter of about 20 nm was prepared using a sol-gel technique¹⁰. Then this xerogel rod was solution doped with the precursor $[\text{Bi}(\text{Hsal})_3(\text{bipy}) \cdot \text{C}_7\text{H}_8]_2$, where $\text{Hsal} = \text{O}_2\text{CC}_6\text{H}_4\text{-2-OH}$. The synthesis of the precursor was described previously¹¹. After the dehydroxylation procedure under chlorine/oxygen atmosphere the samples were sintered at 1300 °C under helium atmosphere resulting in a dense, transparent and colorless monolithic cylindrical preform of 5 mm diameter. This preform was cut and polished to produce the samples with the dimensions of $2 \times 4 \times 5 \text{ mm}^3$. The molar ratio Bi/Si inside the preform was determined by the electron probe microanalysis (EPMA), and it was estimated to be around 300 ppm. The experimental setup for measurements of MCPL is schematically shown in Fig.1. The experiments in the temperature range of 1.45-300 K and MF's in the range of 0-7 T were performed in the closed cycle magneto-optical cryostat (SpectromagPT, Oxford Instr.). The thermal stability of the samples attached to the holder of the variable temperature insert was about of 0.01 K except the range from 4.2 to 10 K where the thermal stability was $\sim 0.05 \text{ K}$. Laser diode or frequency doubled Ti:Sapphire laser were used for the excitation at 375 nm. The signal of MCPL was measured in Faraday geometry (the external MF is paral-

^{a)}Electronic mail: Igor.Razdobreev@univ-lille1.fr

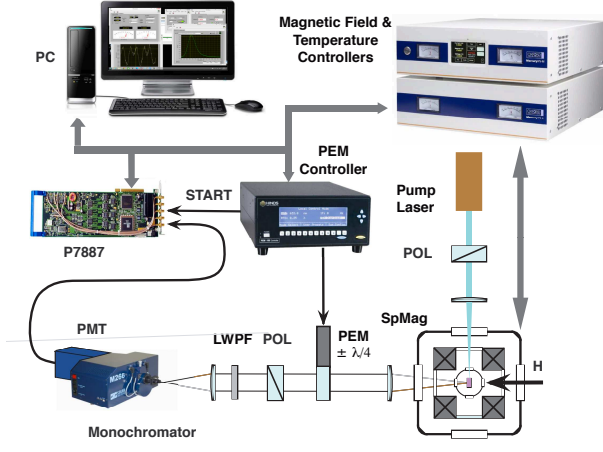


FIG. 1. Experimental setup. SpMag - Oxford Spectro-magPT magneto-optical cryostat; PEM - photoelastic modulator; POL - polarizer; LWPF - long wave pass optical filter; PMT - photomultiplier tube; P7887 - photon counting card (multiscaler).

parallel to vector \vec{k} of emitted photons). The quarter-wave retardation ($\pm\lambda/4$) was introduced by the photoelastic modulator (I/FS-20, Hinds Instr.) at the frequency of 20.077 kHz. The resulting PL emission was analyzed by the fixed linear polarizer (LPNIR100-MP2, Thorlabs), then filtered through a monochromator and detected with the nitrogen cooled InP/InGaAs photomultiplier R5509-73 (Hamamatsu Inc.). The photon counting technique (P7887 scaler, Fast ComTec) was used to record the signal because of its better signal to noise ratio. The spectral resolution in the range of the first ES at 1440 nm was ~ 5 nm and 1.5 nm in the range of 650-950 nm.

The details on the photoluminescence in Bi-doped silica glass without other co-dopant at low temperature (10 K) and at various excitation wavelengths were reported previously⁹. Therefore we show in Fig. 2(a) and 2(b) only the comparison of luminescence and MCPL signals ($I^+ - I^-$) obtained by applying a field of 6 T at 1.48 K in two spectral ranges that correspond to the first (1350-1550 nm) and to the third ES's (650-890 nm). In the range of the second ES (900-940 nm) we did not detect any MCPL signal. The MCPL spectrum reveals that the band around 830 nm consists of three components. The most intense one exhibits positive MCPL signal, $I^+ - I^- > 0$, with corresponding peak value of $\Delta_{\text{MCPL}} = +0.0095$ measured at 830 nm. Two other bands are seen in the MCPL as side bands with $I^+ - I^- < 0$. The MCPL band at 1440 nm has a much simpler form with negative sign in the whole measured wavelength range. The corresponding peak value is $\Delta_{\text{MCPL}} = -0.28$ in the MF of 6 T at 1.48 K. Both MCPL bands (the principal in the case of 830 nm band), are blue- and red-shifted compared to the corresponding luminescence bands (see Fig. 2). Moreover, this shift is more pronounced on the one side, short-wavelength for the band at 1440 nm and long-wavelength for the band at 830 nm. It is straight-

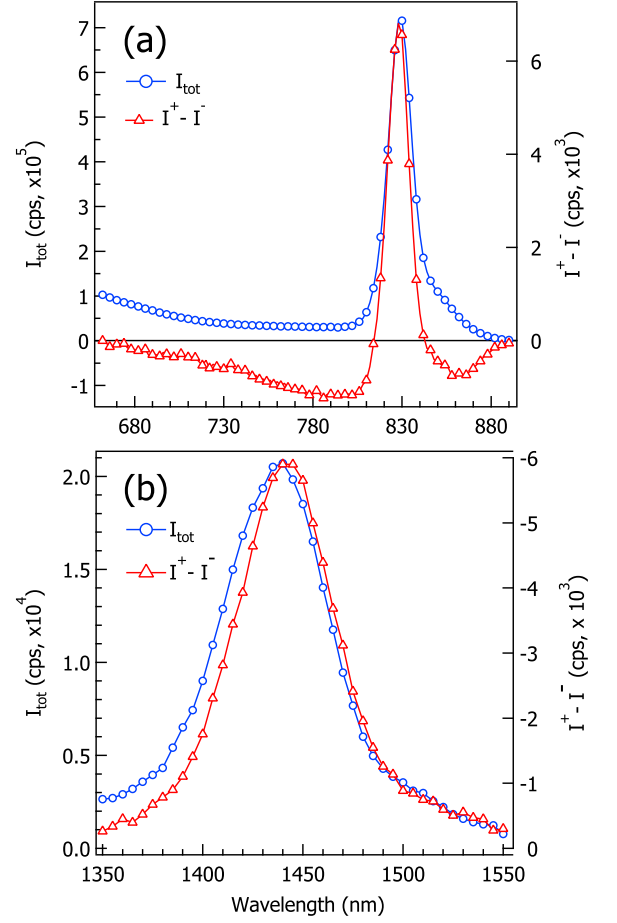


FIG. 2. Spectra of the total (I_{tot}) and MCPL ($I^+ - I^-$) intensities corresponding to the third (a) and first (b) excited states of the luminescent center in Bi-doped silica glass. $T = 1.48$ K, $B = 6$ T, $\lambda_{\text{exc}} = 375$ nm, $P_{\text{exc}} = 7$ mW. (c) Magnetic field dependences of Δ_{MCPL} as a function of $\mu_B B/k_B T$. (d) Temperature dependence of Δ_{MCPL} at various MF's. Markers and solid lines correspond to experimental data and to the global fit, respectively. $\lambda_{\text{det}} = 1440$ nm.

forward to show that at very low temperatures and high fields such behavior can be assigned to the contribution in Δ_{MCPL} of the term which has the linear spectral dependence. The only term exhibiting a spectral dependence is the \mathcal{A} -term which for the case of MCPL is due to the transitions to Zeeman components of the GS¹². The \mathcal{A} -term contribution should be approximately zero at the spectral band maximum^{12,13} that allows to simplify significantly the investigation of the effects of MF and temperature. Below we consider the field and temperature dependences of Δ_{MCPL} only at the peak wavelength of the total luminescence I_{tot} of the first ES at 1440 nm. Fig. 3(a) shows the MF dependences of Δ_{MCPL} plotted as a function of $\mu_B B/k_B T$ at fixed temperatures, where μ_B is the Bohr magneton, and k_B is the Boltzmann constant. It is seen that there is no superposition and the isotherms exhibit nesting behavior. Fig. 3(b) displays the tempera-

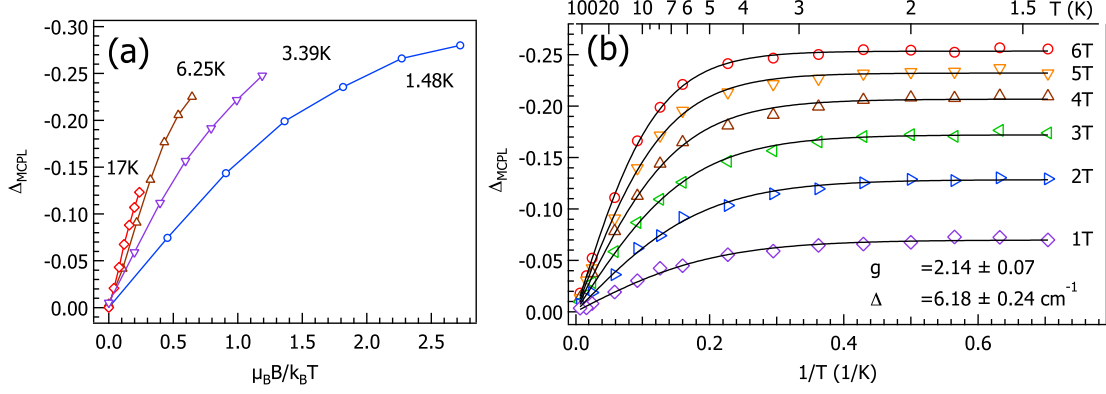


FIG. 3. a) Magnetic field dependences of Δ_{MCP} as a function of $\mu_B B / k_B T$. d) Temperature dependence of Δ_{MCP} at various MF's. Markers and solid lines correspond to experimental data and to the global fit, respectively. $\lambda_{\text{det}} = 1440 \text{ nm}$.

ture dependences of Δ_{MCP} plotted as a function of $1/T$ at fixed MF's. It is seen that the saturation values of Δ_{MCP} are different for each field. Magnetic saturation occurs within a paramagnetic state when the higher lying levels are depopulated due to the field splitting or due to the temperature decrease. For an isolated Kramers doublet (systems with unpaired electron) we expect to observe the field independent limit for the Δ_{MCP} and the unique curve when the latter is plotted as a function of $\mu_B B / k_B T$. If there is an additional level (from another Kramers doublet, for example) in a close proximity to the lowest one, then due to the field-induced mixing the \mathcal{B} -term appears and can result in the behavior similar to that shown in Fig. 2(a) but the character of the saturation curves plotted as a function of $1/T$ remains very different from that shown in Fig. 2(b). The same conclusion follows from a consideration of the case when the transition contains the so-called z -polarization¹⁴ and the effects of both g_{\perp} and M_z / M_{xy} , the ratio of the z -polarized to the xy -polarized transition dipole moments, are taken into account.

On the other hand, for the systems with a zero-field splitting (non-Kramers, even electron systems), the changes in the population of higher levels should affect the MCP intensity leading to the nesting of saturation magnetization curves taken at different temperatures in accordance with Fig. 3(a). Alternatively, plotting the temperature dependence at constant field separates the temperature and field effects as it is shown in Fig. 3(d). Fig. 4 illustrates two non-exhaustive examples of the energy level diagrams corresponding to this kind of systems. Both examples contain all necessary ingredients to explain all the observed features in the behavior of Δ_{MCP} . The ES of the system shown in Fig. 4(a) is a spin-triplet state and the GS is also a spin triplet. Though we consider below only this particular example, the result is identical to the case of the spin-quintet ES show in Fig. 4(b). The analysis of the saturation curves for such a system can be performed in terms of the spin

Hamiltonian with the axial (D) and rhombic (E) zero-field splitting parameters¹⁵:

$$\mathcal{H} = D \left\{ S_z^2 - \frac{1}{3} S(S+1) \right\} + E (S_x^2 - S_y^2) + g_{\parallel} \mu_B B S_z \cos \theta, \quad (1)$$

where θ is the angle between the MF and the axis of symmetry (z -axis), and which implies $g_{\perp} \ll g_{\parallel}$.

First, the triplet ES is split by the axial component $D < 0$ that brings the doublet $m_s = \pm 1$ in lowest position. The rhombic component further removes the degeneracy ($\Delta = 2E$), and the condition $\Delta \ll |D|$ ensures its isolated character. Without an external MF the spin Hamiltonian is diagonalized with the real wavefunctions $\psi^{\pm} = 1/\sqrt{2}(|1\rangle \pm |\bar{1}\rangle)$. It is clear that the angular momentum is quenched and there is no circularly polarized emission. The MF appears as an off-diagonal pure imaginary perturbation $g_{\parallel} \mu_B B \cos \theta$. This Zeeman perturbation changes the wavefunctions and now they take the form: $\psi_H^+ = \cos \alpha |1\rangle + \sin \alpha |\bar{1}\rangle$ and $\psi_H^- = \sin \alpha |1\rangle - \cos \alpha |\bar{1}\rangle$, where $\tan 2\alpha = \Delta/2G$ and $G = g_{\parallel} \mu_B B \cos \theta$ ¹⁵.

The described behavior is quite similar to that observed in MCD for the isolated non-Kramers doublet¹⁴. To use the corresponding analytical expression derived for the case of MCD it must be corrected for MCP by taking into account the effect of photoselection according to Schatz et al.¹³. The resulting formula which describes the temperature and MF dependences of Δ_{MCP} in a disordered system is:

$$\Delta_{\text{MCP}} = A_{\text{sat}} \int_0^1 \frac{2n^4 G_z}{\sqrt{\Delta^2 + 4n^2 G_z^2}} \tanh \left(\frac{\sqrt{\Delta^2 + 4n^2 G_z^2}}{2kT} \right) dn, \quad (2)$$

where $G_z = g_{\parallel} \mu_B B$ and $n = \cos \theta$. This equation is valid to describe the behavior of the MCP from the strongly anisotropic non-Kramers doublet with $g_{\perp} \ll g_{\parallel}$ and $M_z / M_{xy} = 0$. The nonzero g_{\perp} and M_z / M_{xy} could be taken into account also, however, the additional parameters will soften the overall fit without affecting the main

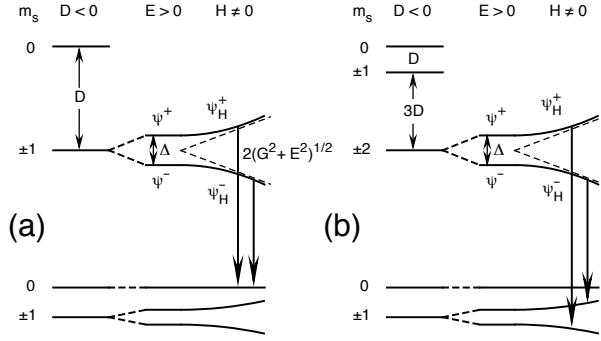


FIG. 4. Energy level diagram to explain the temperature and field dependent effects in MCPL. (a) Spin-triplet ground state and isolated non-Kramers doublet from the spin-triplet $S = 1$ excited state; (b) Same as in (a), but ES is spin-quintet. All splittings are exaggerated. See text.

conclusions. The simultaneous fit of all curves shown in Fig. 2(d) by simulated annealing method¹⁶ results in $g_{\parallel} = 2.14 \pm 0.07$ and $\Delta = 6.18 \pm 0.24 \text{ cm}^{-1}$. The obtained value of g -factor indicates that the first excited can not be put in correspondence to the 3P_1 state of the isolated Bi^+ ion for which we expect $g \leq 1.5$. It must be emphasized that the proposed energy level diagrams are non-exhaustive because our experiment does not reveal neither the exact multiplicity nor the character of the lowest spin component of the GS. Nevertheless, by simple evaluation of the population ratio in the ES we can conclude that the contribution of the \mathcal{C} -term in the described above spectral shift of MCPL band is negligible. Then this shift is due to the \mathcal{A} -term, as a consequence, the GS of the luminescent center is a magnetic multiplet and this is the second important finding in our experiment. This again eliminates isolated Bi^+ ion as a possible luminescent center. It worth noting here, that regardless what spin sublevel of the GS is lowest, in the frame of the presented model the ESR is inaccessible. For instance, if $m_s = \pm 1$ (or $m_s = \pm 2$) is lowest sublevel of GS, one can expect that the condition $|D| \gg \Delta$ is also valid while the splitting of the GS doublet is at least comparable to the ES one. This explains the fact that even “forbidden” electron spin resonance with $\Delta m_s = \pm 2$ in Bi-doped glasses could not be detected in X-band (the photon energy $\approx 0.33 \text{ cm}^{-1}$).

Sokolov et al.^{17,18} proposed first Bi_2^{2+} and Bi_2^{2-} dimers then the complexes of divalent bismuth with neutral oxygen vacancies $\text{Bi}^{2+} - \text{V}_\text{O}$ to explain the NIR PL observed in Bi-doped glasses. It should be clear from the above discussion that Bi_2^{2-} dimers with unpaired electron cannot be responsible for the observed temperature dependence of MCPL. In the recently proposed model of $\text{Bi}^{2+} - \text{V}_\text{O}$ the first ES is a perfectly isolated Kramers doublet (see Fig. 3 in Ref.¹⁸). Thus, this model is also inconsistent with our experiment. In the model of Bi_2^{2-} all emitting states are singlet while the GS is a triplet (see Fig. 2 in Ref.¹⁷). In such a system only \mathcal{A} -term can appear in the MCPL. However, this term is temperature independent and it

can exhibit only the linear field dependence¹². It follows that the model of isolated Bi_2^{2-} dimers is also inconsistent with our experimental observations. In all above mentioned models the GS is a spin multiplet that implies that ESR in principle can be observed. Though Khonthon et al.¹⁹ reported on the observation of an ESR signal with $g \approx 2.2$, its assignment to some luminescent center cannot be unambiguous without additional experiments. On the contrary, our experiment directly connects the particular luminescence band to the paramagnetic properties of the luminescent center. Finally, Dianov²⁰ among other possible origins of NIR PL in Bi-doped silica suggested $\text{Bi}^{2+} - \text{Bi}^{3+}$ dimer and Bi^+ ion between two neutral vacancies. If the first one is again the system with unpaired electron, the latter one should be considered at least in the frame of molecular orbitals because the GS of the isolated Bi^+ ion is a singlet.

In conclusion, MCPL in Bi-doped silica glass was investigated in a wide temperature and MF ranges. It was found that the photoluminescence from the first ES (lasing level) exhibits a strong magnetic circular polarization. The experiments put in evidence the spin multiplicity of the ES and GS of the luminescent center. The field and temperature dependences of the MCPL signal recorded at 1440 nm rule out the odd-electron system as a possible origin of the NIR photoluminescence. This correlates well with the known experimental fact that ESR cannot be observed neither in the GS nor in the ES with the standard method. The results of the experiment can be explained in the assumption that the NIR PL originates from an isolated non-Kramers doublet (ES) and the GS is the spin-triplet or spin-quintet state of the even-electron luminescent center.

FUNDING INFORMATION

“Agence Nationale de la Recherche”, grant ANR “BOATS” 12BS04-0019-01.

ACKNOWLEDGMENTS

I.R. is grateful to L.F. Chibotaru for reading the manuscript and his comments.

- ¹I. A. Bufetov and E. M. Dianov, *Laser Phys. Lett.* **6**, 487–504 (2009).
- ²K. Murata, Y. Fujimoto, T. Kanabe, H. Fujita, M. Nakatsuka, *Fusion Eng. Des.* **44**, 437–439 (1999). Volume = 44, Year = 1999
- ³Y. Fujimoto and M. Nakatsuka, *Jpn. J. Appl. Phys.* **40**, L279 – L281 (2001).
- ⁴M. Peng, G. Dong, L. Wondraczek, L. Zhang, N. Zhang, N. and J. Qiu, *J. Non-Cryst. Solids* **357**, 2241–2245 (2011).
- ⁵E. M. Dianov, *Light: Science & Applications* **1**, 1–7 (2012).
- ⁶P. J. Stephens, *Annu. Rev. Phys. Chem.* **25**, 201–232 (1974).
- ⁷J. P. Riehl and F. S. Richardson *J. Chem. Phys.* **65**, 1011–1021 (1976).
- ⁸R. Serber, *Phys. Rev.* **41**, 489–506 (1932).
- ⁹I. Razdobreev, H. El Hamzaoui, V. Yu. Ivanov, E. F. Kustov, B. Capoen, and M. Bouazaoui, *Opt. Lett.* **35**, 1341–1343 (2010).

- ¹⁰H. El Hamzaoui, L. Courthoux, V. N. Nguyen, E. Berrier, A. Favre, L. Bigot, M. Bouazaoui, and B. Capoen, *Mater. Chem. Phys.* **121**, 83 – 88 (2010).
- ¹¹J. H. Thurston, E. M. Marlier, and K. H. Whitmire, *Chem. Commun.* **23**, 2834–2835 (2002).
- ¹²V. S. Zapasskii and P. P. Feofilov, *Sov. Phys. Uspekhi* **18**, 323–342 (1975).
- ¹³P. N. Schatz, R. L. Mowery, and E. R. Krausz, *Mol. Phys.* **35**, 1537–1557 (1978).
- ¹⁴E. I. Solomon, E. G. Pavel, K. E. Loeb, and C. Campochiaro, *Coordin. Chem. Rev.* **144**, 369–460 (1995).
- ¹⁵A. Abragam and B. Bleaney, *Electron Paramagnetic Resonance of Transition Ions* (Oxford University Press, London, 1970).
- ¹⁶W. H. Press, S. A. Teukolsky, W. T. Vetterling, and B. P. Flannery, *Numerical Recipes in C. The Art of Scientific Computing* (Cambridge University Press, NY, 1992).
- ¹⁷V. O. Sokolov, V. G. Plotnichenko, and E. M. Dianov, *Opt. Lett.* **33**, 1488–1490 (2008).
- ¹⁸V. O. Sokolov, V. G. Plotnichenko, and E. M. Dianov, *Opt. Mater. Express* **5**, 163–168 (2015).
- ¹⁹S. Khonthon, S. Morimoto, Y. Arai, and Y. Ohishi, *J. Ceram. Soc. Jpn.* **115**, 259–263 (2007).
- ²⁰E. M. Dianov, *Quantum Electron.* **40**, 283–285 (2010).